(15) Llopis, J.; Subirana, J. A. *J. Colloid Sci.* **1961**, *16*, 618.
(16) Jaffé, J.; Berliner, C.; Lambert, M. *J. Chem. Phys.* **1967**, *64*, 499.
(17) Kawaguchi, M.; Yoshida, A.; Takahashi, A. *Macromolecules* **1983**, *16*, 956.
(18) Vilanove, R.; Rondelez, F. *Phys. Rev. Lett.* **1980**, *45*, 1502.
(19) Duplantier, B.; Saleur, H. *Phys. Rev. Lett.* **1987**, *59*, 539.
(20) Vilanove, R.; Poupinet, D.; Rondelez, F. *Macromolecules* **1988**, *21*, 2880.
(21) Poupinet, D.; Dêtry, D.; Vilanove, R.; Rondelez, F., to be submitted for publication.
(22) Weill, G.; des Cloizeaux, J. *J. Phys. (Les Ulis, Fr.)* **1979**, *40*, 99.
(23) des Cloizeaux, J.; Jannink, G. Les Polymères en Solution. *Editions de Physique*; 1987.

Solution Properties of Amine-Cured Epoxy Resins Based on Triglycidyl Isocyanurate: Semidilute Solutions

E. Wachenfeld-Eisele and W. Burchard*

Institute of Macromolecular Chemistry, Stefan-Meier-Strasse 31, University of Freiburg, 7800 Freiburg i.Br., Federal Republic of Germany. *Received August 8, 1988; Revised Manuscript Received November 30, 1988*

ABSTRACT: The properties of epoxy resins, prepared by the curing reaction of triglycidyl isocyanurate (TGI) with hexamethylenediamine (HMDA), have been studied in semidilute solution. Because of its ambiguity, the commonly used definition of the coil overlap concentration c^* is avoided, and the thermodynamically clearly defined parameter $X = A_2M_wc$ is instead used as a scaling parameter. The reduced osmotic modulus $(M_w/RT)(\partial\pi/\partial c) = M_wKc/R_{\theta=0}$ of four high molecular weight samples was obtained by extrapolation to $\theta = 0$. The lowest molecular weight sample shows behavior between that of flexible random coils and hard, impenetrable spheres, as was expected, but the curves are shifted toward smaller X values the larger the molecules. This unexpected behavior is tentatively explained by the strong decay of A_2 with growing cluster size and extreme polydispersity. The four curves form, however, asymptotically one common line when $c[\eta]$ is used as a scaling parameter. Similarly a master curve is found for the zero shear rate viscosity when $c[\eta]$ is used. The final exponent $n = 2.4 \pm 0.1$ agrees very satisfactorily with the general relationship $na = 0.75$ that was recently predicted for randomly branched materials, where $a \simeq 0.30$ is the exponent in the Mark-Houwink equation. This exponent is close to 0.375 as was predicted by the percolation theory. The concentration dependence of the translational diffusion coefficient $D(c)$ is significantly weaker than that for impenetrable spheres. $D(c)$ contains a thermodynamic part and a counteracting frictional part. Since the thermodynamic part was measured by static light scattering, the frictional contribution is considered separately. The strongly increasing friction of these randomly branched samples is much more pronounced than for spheres. Because of the lack of theory, even for hard spheres, these phenomena cannot so far be quantitatively interpreted.

Introduction

Reaction of triglycidyl isocyanurate (TGI, Figure 1) with 1,6-hexanediamine (HMDA) yields statistically branched epoxy resins with a high branching density and a very broad molecular weight distribution. The dilute solution properties of these resins have been discussed in previous papers.[1,2] This paper deals with static (SLS) and dynamic (DLS) light-scattering and viscosity measurements of *semidilute solutions* of TGI/HMDA resins with weight-average molecular weights M_w of about 2×10^6–5×10^6 g/mol.

During the past few years much experimental work has been carried out with light scattering from semidilute solutions, mainly on linear chains.[3-9] Recently other studies on different architectures[9-14] have also been performed. A characteristic feature of semidilute solutions of linear chains is that all properties become molecular weight independent.[8] However, recent studies with other types of polymers reveal that the properties depend on the architecture.[9] Theoretical predictions exist so far only for flexible, linear chains in marginal to good solvents and for hard spheres at high concentrations. These theories are not discussed in detail here because of their complexity, and we refer to the literature.[15-20] Since no theory exists for randomly branched polymers, the results of the measurements are compared to these two theories. The discussion is subdivided into five parts: (i) osmotic modulus, (ii) M_w dependence of the second virial coefficient, (iii) viscosity measurements, (iv) diffusion coefficient, and (v) anomalies at high concentration.

Experimental Section

1,6-Hexanediamine from Sigma was used without further purification. Triglycidyl isocyanurate (Araldit PT 810 from Ciba Geigy) is a mixture of two enantiomer pairs (RRS/SSR or α-TGI and RRR/SSS or β-TGI). The less symmetric α-TGI, which was used for the synthesis of the epoxy resins, was obtained by fractional crystallization from this mixture.

Crystallization of α-TGI. A mixture of α- and β-TGI was refluxed in methanol (TGI:methanol 1:4 by weight) for 10 min and filtered hot over a hot Buchner funnel. α-TGI separates from the filtrate as fine white crystals when the solution is cooled to 0 °C. The crystalline α-TGI was filtered off, washed with cold methanol, and then dried in vacuo for 2–3 days at room temperature. The resulting product had a melting point of 105–106 °C (lit.[21] mp 106 °C).

Synthesis of the Resins. All resins were prepared in dimethylformamide (DMF) solution in calibrated flasks. The concentration was chosen so that 1.7 mmol monomer was diluted in 1 mL of DMF. To make resins of different molecular weight, the composition was changed slightly. The appropriate amount of TGI was placed in a calibrated flask, and DMF was added. The flask then was immersed in an oil bath of 70 °C and TGI dissolved. With a pipet the necessary amount of HMDA (in DMF) was added. Then the solution was maintained at 70 °C for 20 h, cooled to room temperature, and filled to the marker with DMF.

Refractive Index Increment. The refractive index increments were measured in DMF at 20 °C with a Brice Phoenix differential refractometer.

Light-Scattering Measurements. Static and dynamic light scattering (SLS and DLS) was measured simultaneously in DMF at 20 °C with an automatic goniometer and a structurator/correlator ALV-3000 by ALV-Langen. The blue line ($\lambda_0 = 488$ nm) of an argon ion laser Model 2000 by Spectra Physics was used

0024-9297/89/2222-2496$01.50/0 © 1989 American Chemical Society

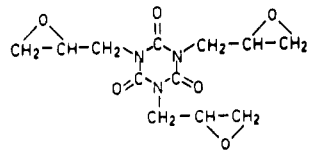

Triglycidyl isocyanurate (TGI)

Figure 1. Chemical formula of triglycidyl isocyanurate.

as light source. The correlator was coupled to a Victor-Sirius personal computer where the data were treated on-line with the program ODIL by Eisele.[22] Most measurements were carried out in the "linear τ mode". The "sample time" was determined separately for each sample and changed automatically with the changing measuring angle. In "multiple τ mode" the sample time was always 1 μs. To make the solutions dust free, the measuring cells were "floated"[23] in an ultracentrifuge (L5-50B, Beckmann) at 10000 rpm for 30 min. The diffusion coefficient was determined from the first cumulant of a three-cumulant fit of the autocorrelation function.

Viscosity Measurements. In dilute solution [η] was measured in DMF at 20 °C in an automatic Ubbelohde viscometer by Schott. Measurements in semidilute DMF solution (20 °C) were carried out in a Haake Rotovisko RV100 with measuring systems CV100 and ME30.

Results and Discussion

Dealing with different polymer architectures at high concentrations, we first have to clarify the term "semidilute solution". It has to be emphasized that even for flexible, linear chains there exists no *exact* definition for an overlap concentration c^* that defines a semidilute solution. In dilute solution coils interpenetrate only partly and show essentially equivalent hard-sphere behavior, but in semidilute solution these coils overlap and form an entangled, transient network. The most common definitions of c^* are given in eq 1–3.[24,25] They may differ by a factor of about 10. In eq 1–3, M is the molecular weight of the polymer, N_A Avogadro's number, and R_g and R_h the radius of gyration and the hydrodynamic radius, respectively.

$$c^* = [\eta]^{-1} \tag{1}$$

$$c^*_{R_g} = (3M)/(4\pi N_A R_g^3) \tag{2}$$

$$c^*_{R_h} = (3M)/(4\pi N_A R_h^3) \tag{3}$$

For more dense architectures, e.g., randomly branched epoxy resins, the whole concept of semidilute solutions becomes questionable, since no full interpenetration can occur, and for hard spheres no interpenetration at all is possible.

(i) Osmotic Modulus. For the above reason it is necessary to find a suitable parameter on the basis of thermodynamics rather than on geometry. Such a parameter is given by the osmotic modulus, which is defined via the scattering intensity at zero angle[26]

$$R_{\theta=0} = KcS(0,c) \tag{4}$$

where R_θ is the Rayleigh ratio, $K = (4\pi^2 n_0^2 (dn/dc)^2)/(N_A \lambda_0^4)$ is the optical constrast constant for vertically polarized light, and c is the concentration of polymer. According to the fluctuation theory of Smoluchowski[27] and Einstein[28] the structure factor $S(0,c)$ at zero angle is defined by thermodynamics, i.e., by the osmotic compressibility:

$$S(0,c) = RT(\partial c/\partial \pi) \tag{5}$$

This value can be obtained by SLS (see eq 4). If eq 4 is normalized with respect to the molecular weight of the particle, the dimensionless relationship

$$M_w Kc/R_{\theta=0} = (M_w/RT)(\partial \pi/\partial c) \tag{6}$$

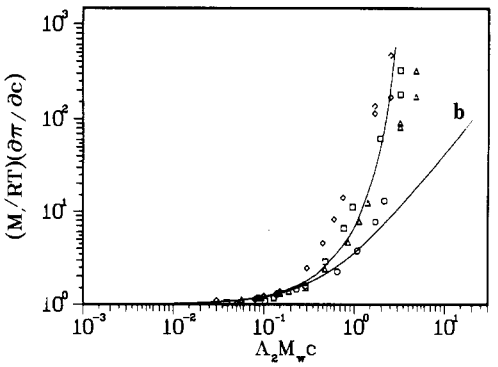

Figure 2. Osmotic modulus as a function of $X = A_2M_wc$. (—) (a) Theory for hard spheres. (b) Theory for flexible chains, TGI/HMDA resins with molecular weight M_w (□) 5.28 × 10^6, (◇) 4.12 × 10^6, (△) 3.00 × 10^6, and (○) 2.30 × 10^6 g/mol.

is obtained, which in the following will be named the "reduced osmotic modulus".

For moderate concentrations the osmotic pressure can be expanded in a virial series which gives for eq 6

$$(M_w/RT)(\partial \pi/\partial c) = 1 + 2A_2M_w = 3A_3M_wc^2 + \ldots \tag{7}$$

and this in turn can be written as follows:[29]

$$(M_w/RT)(\partial \pi/\partial c) = 1 + 2X + 3a_3X^2 + 4a_4X^3 + \ldots \tag{8}$$

where $X = A_2M_wc$. This parameter has a simple meaning for hard spheres for which[30]

$$X = A_2M_wc = 4(V/M_w)c = 4(c/c^*) \tag{9}$$

where $c^* = V/M_w$ with V the molar volume of the sphere. For linear, flexible chains, on the other hand, this parameter is[31]

$$X = A_2M_wc = (4\pi^{3/2}N_AR_g^3c)/M_w\psi(z) \tag{10}$$

where z is the common interaction parameter. The interpenetration function $\psi(z)$ for weak interaction ($z \simeq 1$) already approaches a constant value of about 0.24 ± 0.02 (ref 15 and 17), and this allows us to write

$$X = 4(V_{eq}/M_w)c \tag{11}$$

where

$$V_{eq} = 0.24\pi^{3/2}N_AR_g^3 \tag{12}$$

is the equivalent hard-sphere radius.

For star-branched molecules eq 10 can be used, but the interpenetration decreases and $\psi(z\to\infty)$ increases.[32] It may be emphasized that X is a thermodynamically well-defined scaling parameter and includes both different molecular weights and different solvent qualities in addition to the concentration dependence. The differences in architecture show their influence in the values of the coefficients a_3 and a_4 (eq 8) or more generally in the shape of the reduced osmotic modulus as a function of X. Because of this behavior X is also used tentatively for the randomly branched resins.

Figure 2 shows the results of the measurements on TGI/HMDA resins with molecular weights of 2.3 × 10^6, 3.0 × 10^6, 4.1 × 10^6, and 5.3 × 10^6 g/mol in DMF at 20 °C. For comparison, the theoretical curves for hard spheres by Carnahan and Starling[19] and for linear, flexible chains by Ohta and Oono[16] (derived from renormalization group theory) are presented in this plot. The lowest molecular weight sample lies as expected between these two limiting curves, since these hyperbranched molecules can interpenetrate only weakly and thus may resemble hard spheres. The curves for the higher molecular weights

display similar shape but are shifted toward smaller X values and eventually fall beyond the hard-sphere curve. At first sight, this behavior indicates a stronger repulsion between the resin molecules at high concentrations than is observed for hard, homogeneous spheres. At present, we cannot present a fully satisfying explanation. However, linear chains and these randomly branched resins show strikingly different molecular weight dependences of the second virial coefficient. For linear chains[8,31]

$$A_2 \sim M_w^{-0.2} \tag{13a}$$

and thus

$$X_{lin} \sim M_w^{0.8} c \tag{13b}$$

Experimentally we found for the TGI/HMDA resins

$$A_2 \sim M_w^{-2.9} \tag{14a}$$

$$X_{bra} \sim M_w^{-1.9} c \tag{14b}$$

Because of this very different behavior, the curves of the resins are shifted with increasing M_w strongly to the left in Figure 2, i.e., X_{lin} *increases* with M_w whereas X_{bra} *decreases*.

(ii) M_w Dependence of the Second Virial Coefficient. This fact requires a more detailed consideration of the influence of branching on the second virial coefficient. A decrease of A_2 with branching was observed[32,33] already in 1949 and is theoretically expected.[34,35] For regularly branched structures, e.g., star-branched molecules, one can write[36]

$$\frac{A_{2,bra}}{A_{2,lin}} = \frac{R_{g,bra}^3}{R_{g,lin}^3} \frac{\psi_{bra}(z)}{\psi_{lin}(z)} = g^{3/2} = \frac{\psi_{bra}(z)}{\psi_{lin}(z)} \tag{15}$$

where the shrinking factor g is defined as

$$g = \langle S^2 \rangle_{bra} / \langle S^2 \rangle_{lin} \tag{16}$$

at the same value of M_w. The interpenetration functions ψ_{lin} and ψ_{bra} for sufficiently large z approach constant values.[17,31,36] As already mentioned in section i the ψ_{bra} ($z \to \infty$) has a larger value than ψ_{lin} ($z \to \infty$). The ratio ψ_{bra}/ψ_{lin} appears to reach a constant value of about 4 in the limit of large branching densities. This value is close to the ratio of hard spheres to linear chains $\psi_{sph}/\psi_{lin} = 1.61/0.24 \simeq 6.7$. The shrinking factor g decreases continuously with increasing number of branches.[37] Consequently the second virial coefficient decreases for branched samples of the same molecular weight in comparison to linear chains. For randomly branched structures the situation becomes more complex because of two facts. First, the number of branches, f, increases with M_w, and second, the polydispersity also increases with M_w. For this reason the g factor is a function of the molecular weight, whereas $\psi_{bra}(z)/\psi_{lin}(z)$ approaches a constant value. Under these assumptions a simple estimation gives

$$A_{2,b} \sim M_w^{-1.7} \tag{17}$$

Experimentally an exponent of −2.9 was found (Figure 3). In eq 17 the effect of polydispersity is not explicitly taken into account, and at present there is no theory for it. This polydispersity effect may account for such a higher exponent. Figure 3 shows the molecular weight dependence of A_2. At comparatively low molecular weight the exponent is about −0.55 and decreases only at very large M_w to −2.9, but this strong decay of A_2 with increasing M_w may pass more smoothly downward and will give a slope considerably less than −2.9. We wish to emphasize here that accurate measurements of A_2 become difficult because of the small values obtained (which are in the range of 10^{-6}–10^{-5} mol cm^3 g^{-2}). The low exponent of −0.55 is an indication that the interpenetration function $\psi_{bra}(z)$ has not yet reached the limiting plateau value.

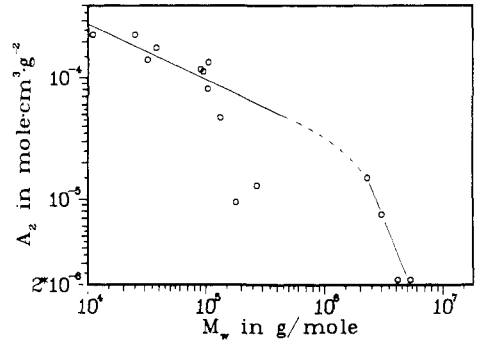

Figure 3. Double-logarithmic plot of the second virial coefficient A_2 against the weight-average molecular weight M_w for TGI/HMDA resins with different molecular weights.

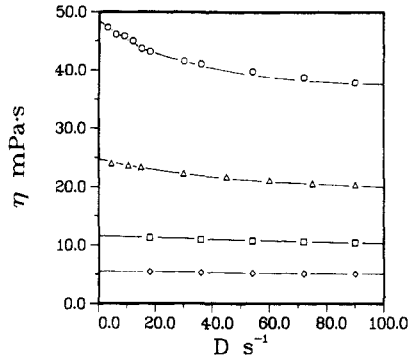

Figure 4. Viscosity as a function of the shear gradient D of a TGI/HMDA sample with $M_w = 5.29 \times 10^6$ g/mol. The concentrations are (◇) 0.0823, (□) 0.1235, (△) 0.1646, and (○) 0.2058 g/mL.

The experimentally observed decrease of X as M_w increases can be interpreted in line with eq 15 by assuming a much stronger decrease of the g factor than predicted by current theories. One possible explanation may be a deswelling which could be caused by excluded-volume shielding or by some incompatibility effects. Preparatively the increase in M_w is achieved by an increase of the epoxy/amine ratio. Although this variation in composition is very small in that high M_w region, it may nevertheless produce a change in the solvation power.

(iii) Viscosity Measurements. For two of the TGI/HMDA resins mentioned with molecular weight M_w of 3.00×10^6 and 5.29×10^6 g/mol, viscosity measurements were carried out in the dilute to semidilute regime. Figure 4 shows the shear gradient dependence of η for different concentrations. As expected the η values increase with increasing concentration as well as with decreasing shear gradient. A double-logarithmic plot of the specific viscosity η_{sp} as a function of $c[\eta]$ ($\eta_{sp} = (\eta_0 - \eta_s)/\eta_s$ with the zero shear rate viscosity $\eta_0 = \lim_{D \to 0} \eta(c)$ and η_s the solvent viscosity) is given in Figure 5. As expected from behavior of linear chains, a universal curve is obtained.

Recent theories on the fractal properties of polymers[38] disclosed, however, significant differences between linear and randomly branched structures. Linear chains exhibit fractal dimensions of $D_s = 1.67$ in the fully swollen and $D = 2.0$ in the Θ state, but the corresponding fractal dimensions for individual (monodisperse) clusters are $D_s = 2.0$ and $D = 2.52$.[39] Furthermore, the random branching process is intimately correlated to the development of a very broad size distribution. In the vicinity of the sol–gel transition, percolation theory predicts for this size distribution behavior $N(m) \sim m^{-\tau} \exp(-m/M_z)$ in which M_z

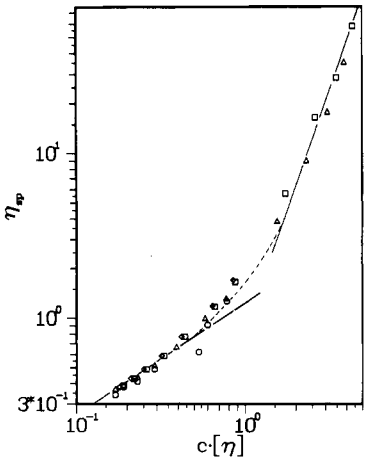

Figure 5. Double-logarithmic plot of the specific viscosity η_{sp} as a function of $c[\eta]$ for TGI/HMDA samples with different molecular weights: (◇) 5.29 × 10^6, (□) 4.12 × 10^6, (△) 3.00 × 10^6, and (○) 2.30 × 10^6 g/mol.

is the z-average molecular weight of the ensemble and $N(m)$ the number of clusters of molecular weight m. The exponent was found to be $\tau = 1 + d/D$, which gives $\tau = 2.2$ for $d = 3$. One particular consequence of this distribution is[38]

$$M_w \sim M_z^{(2D-d)/D} = M_z^{4/5} \tag{18}$$

whereas for common linear polycondensates $M_z/M_w = 1.5$ remains constant as M_w increases. The deviating fractal dimensionality of branched clusters and the mentioned size distribution give rise to remarkably different properties compared to linear chains.[40] Two are relevant in the context of the present findings.

For the intrinsic viscosity in a good solvent Martin et al.[38,40] predict the following behavior in d dimensions:

$$[\eta] \sim M_z^{d(1/D_s-1/D)} = M_z^{3/10} \tag{19a}$$

which with eq 18 gives

$$[\eta] \sim M_w^{3/8} = M_w^{0.375} \tag{19b}$$

For marginal sovents D_s lies closer to D, and the exponent in eq 19b will be even smaller. This prediction agrees well with the experimentally observed exponent of $a \simeq 0.30$.[2] This is quite a different result than found with linear chains where $a \simeq 0.7$–0.8.

Even more striking is the predicted exponent n in the relationship for η_{sp} as a function of $c[\eta] \gg 1$. Martin[41] was able to show for randomly branched structures

$$(na)_{bra} = 3/4 \tag{20}$$

which deviates considerably from the corresponding relationship for linear chains[42] (see Appendix)

$$(na)_{lin} = 3.4 \tag{21}$$

Inserting $a = 0.3$ in eq 20, one finds $n = 2.5$, which is very close to the experimentally observed exponent $n = 2.35 \pm 0.15$.

It still remains striking that for high concentrations the viscosity measurements for different molecular weights form a master curve if $c[\eta]$ is used as the reduced concentration, whereas similar behavior is not observed if A_2M_wc is used. For this reason we conjecture that the quantity $c[\eta]$ might be the better scaling parameter also for the osmotic modulus. Figure 6 demonstrates indeed a good master-curve behavior at high concentrations; for small concentrations, however, A_2M_wc remains the better scaling quantity. An explanation for this behavior cannot yet been offered. We only wish to stress the extremely high

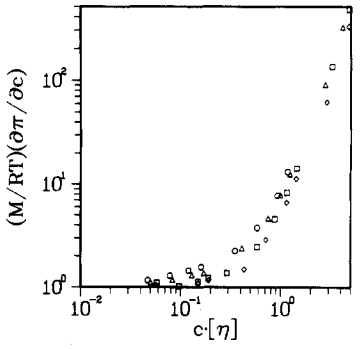

Figure 6. Osmotic modulus as a function of $c[\eta]$ for the TGI/HMDA resins with molecular weight (□) 5.28 × 10^6, (◇) 4.12 × 10^6, (△) 3.00 × 10^6, and (○) 2.30 × 10^6 g/mol.

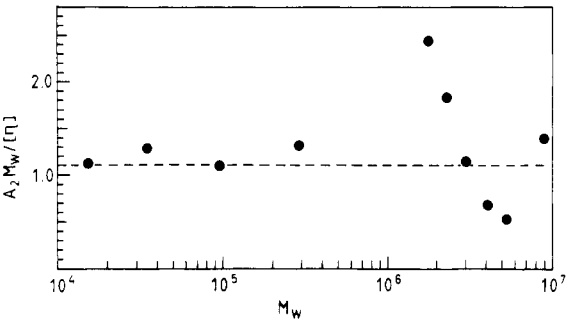

Figure 7. Ratio $A_2M_w/[\eta]$ as a function of M_w for the cured epoxies. The dotted line corresponds to the limiting value for linear chains.

polydispersity of the materials, and the averaging procedure may be significantly different in the dilute and the semidilute regimes.

Recently Daoud and Leibler[43] derived an equation for the osmotic pressure of the form $(M_n/RT)(\pi/c) = f(c/c^*)$. For the osmotic modulus this would give the corresponding relationship $(M_w/RT)(d\pi/dc) = f(c/c^*)$, which is exactly of the form that has been used in eq 8. The authors added, however, a comment that for polydisperse systems $Kc/R_{\theta=0}$ can no longer be expressed by the osmotic modulus since smaller clusters can penetrate into larger ones and will appear swallowed. A rigorous statistical derivation of the consequence of such preferential interpenetration was, however, not given.

We finish the discussion of this section by comparing the dimensionless ratio $A_2M_w/[\eta]$ from these branched samples with those from common linear chains. The result is shown in Figure 7. Taking into proper account of the large experimental error, we may conclude that this ratio increases gradually with increasing molecular weight from the value of 1.1 for linear chains[17,31] to approximately 1.8. At very large M_w a sharp decrease seems to occur which is caused by the observed sharp decrease in A_2. However, more experimental data have to be collected from other branched systems before more definite statements can be made.

(iv) Diffusion Coefficient. The scaling theory of de Gennes[8] predicts two different types of diffusion for the semidilute regime, i.e., diffusion along the contour length of the macromolecule ("reptation") D_{rep} and cooperative diffusion D_{coop}. Reptation should become slower with increasing concentration according to the following power law:[8]

$$D_{rep} \sim (c/c^*)^{-1.75} \tag{22}$$

Cooperative diffusion represents the fast relaxation of the transient network chains and is related to a hydrodynamic correlation length ξ which is often interpreted topologically

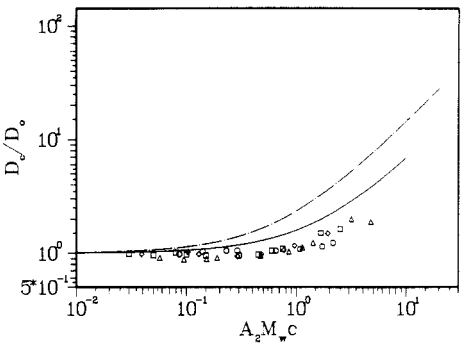

Figure 8. Double-logarithmic plot of the normalized diffusion coefficient at concentration c as a function of X: (-·-) theory for linear, flexible chains; (—) theory for hard spheres, TGI/HMDA resins with different molecular weights. The symbols used are as in Figure 2.

as the chain length between two points of entanglement. With increasing concentration these correlation lengths become shorter and the relaxation faster, following the power law[8]

$$D_{coop} \sim (c/c^*)^{0.75} \tag{23}$$

The scaling predictions give good guidelines for experimentalists on the asymptotic behavior of a system. They have, however, the disadvantage that no clear statements can be derived for the crossover region. The renormalization group theory, on the other hand, is capable of covering the whole concentration regime from dilute to semidilute solutions. Recently Oono and co-workers derived an expression for the coefficient in the linear X term. The following formula is predicted for the dilute *and* semidilute regime:[18]

$$D_c/D_0 = 1 + (e^Y - 3Y/(1 - (1 - \zeta)^{-0.75}))\hat{X} \tag{24}$$

where $Y = \zeta/(8(1 + \zeta))$ and $\zeta = 32z/3$, with z the excluded-volume parameter. For the good solvent limit z and eq 21 take the form

$$\begin{aligned} D_c/D_0 &= 1 + 0.758\hat{X} \quad \text{with} \quad \hat{X} = 1.778X \\ &= 1 + 1.347X \end{aligned} \tag{25}$$

Batchelor predicts a similar formula for the behavior of hard spheres:[20]

$$D_c/D_0 = 1 + 0.333X \tag{26}$$

Figure 8 shows the measured diffusion coefficients for the TGI/HMDA resins of different molecular weight compared to the renormalization group theoretical predictions and to the theory of hard spheres as functions of $X = A_2M_wc$. The experimental curves fall below even the theoretical curve for hard spheres.

Although it is common to interpret the experimental diffusion coefficient curves directly by means of theories, we think that this is not the best procedure. According to irreversible thermodynamics, the diffusion coefficient is given by[31]

$$D_c = (kT/f(c))[(M/RT)/(\partial\pi/\partial c)] \tag{27}$$

where $f(c)$ is the concentration-dependent friction coefficient. The expression in brackets is recognized as the reduced osmotic modulus which was measured by SLS. Therefore the diffusion coefficient contains both a thermodynamic and a hydrodynamic part. Both quantities can be separated by the combination of DLS and SLS. Figure 9 shows a plot of the friction coefficients for the different resins. This curve will not further be discussed, since even for hard spheres the full concentration dependence of the

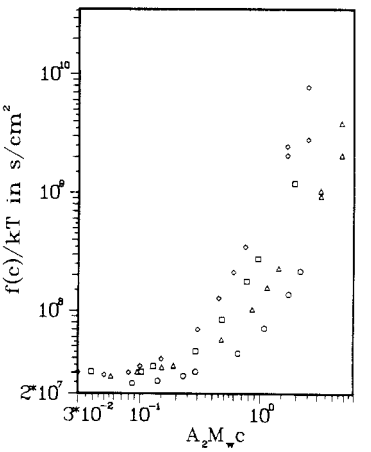

Figure 9. Friction coefficient $f(c)/kT$ as a function of A_2M_wc for the TGI/HMDA samples. Symbols used are as in Figure 2.

friction coefficient is not yet known theoretically. Finally we wish to point out that both the reduced osmotic modulus and the frictional coefficient become significantly nonlinear already close to the overlap concentration while the diffusion coefficient still shows a linear concentration dependence. This demonstrates that this linearity results mostly from a counterbalance of the thermodynamic repulsion and the increase of the fraction when c is increased.

(v) Anomalies at High Concentration. At moderately high concentrations anomalies from the predicted semidilute behavior have often been observed with a number of different polymers. These anomalies are manifested by three effects: (1) Low-angle excess scattering occurs. This is related to a correlation length that is much larger than that of the gel mode.[44] (2) The osmotic modulus shows a turnover, i.e., extrapolating the excess scattering to zero angle, one arrives at an osmotic modulus that clearly lies below the theoretical curve. (3) Simultaneous with 1 and 2 a slow mode of motion appears in the DLS time correlation function.

Since these effects have been observed with so many different architectures,[45] it could be suspected that these anomalies are a general feature. A tentative interpretation of the effects was cluster formation via equilibrium association.

With the TGI/HMDA resins of the present study a low-angle excess scattering is indeed observed at concentrations of about 13% (weak) and 20% (pronounced). On the other hand, this excess low-angle scattering is not as dominating as was observed with other polymers. For this reason no clear turnover in the osmotic modulus is observed, but nevertheless there is a clear deviation from the expected pure entanglement behavior (without association). Possibly the effect may become as drastic as with other polymers at even higher concentrations, which were not measured. For the same reason, a well-separated slow motion could not be observed with these concentrations. A separation of the slow mode from the gellike cooperative diffusion mode will be difficult in these cases anyway, because of the very broad molecular weight distribution of the samples. A clear bimodal behavior of monodisperse samples may apparently now fuse into unimodal behavior.

Concluding Remarks

It may be useful to summarize some of the results with these randomly branched structures.

In contrast to linear, flexible chains, the parameter $X = A_2M_wc$ appears not to be a good scaling parameter for the reduced osmotic modulus. The curves for the different molecular weights no longer form one common line.

The zero shear viscosity of the same samples form a master curve, if $c[\eta]$ is used as a scaling parameter. The asymptotic exponent n at large concentrations is very satisfactorily described by the relationship $na = {}^3/_4$, which differs from the corresponding equation $na = 3.4$ for linear chains where a is the Mark–Houwink exponent of the intrinsic viscosity.

Scaling of the osmotic modulus with $c[\eta]$ leads to a common curve at large concentrations but not at small ones.

The concentration dependence of the diffusion coefficient is even weaker than for hard spheres. This may result from a strong specific hydrodynamic interaction among these macromolecules.

All these effects indicate that the randomly branched structures cannot be described by the renormalization group theory that was developed for linear chains. Measurements with star-branched microgels,[14] which give behavior similar to that described in this paper, confirm the nonapplicability of the existing renormalization group approach.

It appears noteworthy that the *shape* of the osmotic modulus curve appears not to depend significantly on the polydispersity (in agreement with the predictions for linear chains by Oono), but it is clearly a function of the architecture.

Acknowledgment. We are indebted to Dr. James E. Martin for giving us access to his recent theory prior to publication. We thank Dr. Simon B. Ross-Murphy, Unilever Research, Bedford, England, and Professor W. H. Stockmayer, Hanover, NH, for a critical reading of the manuscript and valuable suggestions. W.B. also thanks Dr. M. Budnowski, Henkel KGAA, Düsseldorf, for drawing his attention to the triglycidyl cyanurate reagent, which kindly was given to us by Ciba-Geigy, Basel. The work was financially supported by the Deutsche Forschungsgemeinschaft within the scheme SFB 60.

Appendix: Derivation of Eq 21

For linear chains in the entanglement regime, i.e., $c \gg c^*$, the specific viscosity follows the relationship

$$\eta_{sp} \sim M^{3.4} \tag{A1}$$

On the other hand, the intrinsic viscosity (infinitely diluted solution) follows a Mark–Houwink equation:

$$[\eta] \sim M^a \tag{A2}$$

Replacing M in eq A1 by eq A2, one finds

$$\eta_{sp} \sim [\eta]^{3.4/a} = [\eta]^n \tag{A3}$$

This relationship says nothing about the concentration dependence, which may be weaker than the dependence on $[\eta]$. Experiments give, however, strong evidence that the concentration dependence follows the same power law.

Registry No. (TGI)($H_2N(CH_2)_6NH_2$) (copolymer), 118461-15-7.

References and Notes

(1) Burchard, W.; Bantle, S.; Wachenfeld-Eisele, E. *Makromol. Chem., Macromol. Symp.* **1987**, *7*, 55.
(2) Wachenfeld-Eisele, E.; Burchard, W. In *Biological and Synthetic Polymer Network*; Kramer, O., Ed.; Elsevier: New York, 1988.
(3) Wiltzius, P.; Haller, H. R.; Cannell, D. S.; Schaefer, D. W. *Phys. Rev. Lett.* **1983**, *51*, 1183.
(4) Wenzel, M.; Burchard, W.; Schätzel, K. *Polymer* **1986**, *27*, 195.
(5) Eisele, M.; Burchard, W. *Macromolecules* **1984**, *17*, 1636.
(6) Burchard, W.; Eisele, M. *Pure Appl. Chem.* **1984**, *56*, 1379.
(7) Burchard, W.; Stadler, R.; Freitas, L. L.; Möller, M.; Omeis, J.; Mühleisen, E. In *Biological and Synthetic Polymer Network*; Kramer, O., Ed.; Elsevier: New York, 1988.
(8) de Gennes, P.-G. *Scaling Concepts in Polymer Physics*; Cornell University Press: Ithaca, New York, 1979.
(9) Burchard, W. *Makromol. Chem. Macromol. Symp.* **1988**, *18*, 1.
(10) Delay, M.; Tardieu, A. *Nature* **1983**, *30L*, 415.
(11) Delay, M.; Gromiec, A. *Biopolymers* **1983**, *22*, 1203.
(12) Huber, K.; Burchard, W.; Fetters, L. J. *Polymer* **1987**, *28*.
(13) Coviello, T.; Burchard, W., Dentini, M.; Crecenzi, *Macromolecules* **1987**, *20*, 1102.
(14) Lang, P.; Burchard, W., to be submitted for publication.
(15) Oono, Y. *Adv. Chem. Phys.* **1985**, *61*, 301.
(16) Ohta, T.; Oono, Y. *Phys. Lett.* **1983**, *79*, 339.
(17) Freed, K. F. *Renormalization Group Theory of Macromolecules*; Wiley: New York, 1987.
(18) Oono, Y.; Baldwin, P. R.; Ohta, T. *Phys. Rev. Lett.* **1984**, *53*, 2149.
(19) Carnahan, N. F.; Starling, K. E. *J. Chem. Phys.* **1969**, *51*, 635.
(20) Batchelor, G. K. J. *J. Fluid Mech.* **1976**, *52*, 245.
(21) Budnowski, M. *Angew. Chem., Int. Ed. Engl.* **1968**, *7*, 827.
(22) Eisele, M. Ph.D. Thesis, Freiburg, 1988.
(23) Dandliker, W. B.; Kraut, J. *J. Chem. Phys.* **1955**, *78*, 2380.
(24) Utracki, L.; Simha, R. *J. Polym. Sci., Part A* **1963**, *1*, 1089; *J. Chem. Phys.* **1963**, *67*, 1052.
(25) A modification of the model de Gennes used in ref 8.
(26) (a) Debye, P. *Ann. Phys. (Leipzig)* **1915**, *46*, 809. (b) Debye, P. *Phys. Z.* **1930**, *31*, 419.
(27) Smoluchowski, M. *Ann. Phys.* **1908**, *25*, 205.
(28) Einstein, A. *Ann. Phys.* **1910**, *33*, 1275.
(29) This relationship has been used to terms of X^2 for many years by several authors: Flory, P. J. *Principles of Polymer Chemistry*; Cornell University Press: Ithaca, NY, 1953. Des Cloiseau, J. *J. Phys. (Les Ulis, Fr.)* **1975**, *36*, 281. de Gennes[8] extended this truncated virial expansion and assumed even for $X > 1$ the osmotic pressure being a function of X alone.
(30) Friedman, H. L. *A Course in Statistical Mechanics*: Prentice-Hall: Englewood Cliffs, NJ, 1985.
(31) Yamakawa, H. *Modern Theory of Polymer Solution*; Harper & Row: New York, 1971.
(32) Thurmond, C. D.; Zimm, B. H. *J. Chem. Phys.* **1949**, *17*, 1301.
(33) Doty, P.; Brownstein, M.; Schlener, W. *J. Phys. Colloid Chem.* **1949**, *53*, 213.
(34) Stockmayer, W. H.; Fixman, M. *Ann. N.Y. Acad. Sci.* **1953**, *57*, 334.
(35) Casassa, E. F. *J. Chem. Phys.* **1962**, *37*, 2176; **1964**, *41*, 3213.
(36) Douglas, J. F.; Freed, K. F. *Macromolecules* **1984**, *17*, 1854.
(37) Zimm, B. H.; Stockmayer, W. H. *J. Chem. Phys.* **1949**, *17*, 1301.
(38) Daoud, M.; Martin, J. E. In *The Fractal Approach to Heterogeneous Chemistry: Surfaces, Colloids, Polymers*, Aunir, D., Ed., to be submitted for publication.
(39) Stauffer, D. *Introduction to Percolation Theory*; Taylor & Francis: London, 1985.
(40) Martin, J. E.; Adolf, D.; Wilcoxon, J. P., submitted for publication in *Phys. Rev. A*.
(41) Martin, J. E., personal communication.
(42) Ferry, J. D. *Vicoelastic Properties of Polymers*, 3rd ed.; Wiley: New York, 1983, and other textbooks of polymer chemistry.
(43) Daoud, M.; Leibler, L. *Macromolecules* **1988**, *21*, 1497.
(44) Koberstein, J. T.; Picot, C.; Benoit, H. *Polymer* **1985**, *26*, 673.
(45) Burchard, W. *Makromol. Chem., Macromol. Symp.* **1988**, *18*, 1 there further literature.